Vibrons in a one-dimensional lattice of hydrogen-bonded peptide units: Influence of the inhomogeneous mass distribution in the amino acid sequence

Vincent Pouthier*
Laboratoire de Physique Moléculaire, UMR CNRS 6624, Faculté des Sciences–La Bouloie, Université de Franche-Comté, 25030 Besançon Cedex, France
(Received 25 February 2005; published 6 September 2005)

The influence of the inhomogeneous mass distribution in the amino acid sequence on amide-I vibrons in α-helices is studied within the small polaron approach in a one-dimensional (1D) model. It is shown that inhomogeneities in the sequence favor a randomness in the polaron Hamiltonian via the dressing mechanism. The polaron dynamics is thus described by a 1D tight binding model with correlated off-diagonal disorder. At low temperature, the polaron hopping constants exhibit small fluctuations around a large average value so that the polaron Hamiltonian appears weakly disordered. Extended states occur over a wide range of energies around the band center whereas the states close to the band edges appear localized. By contrast, at biological temperature, a stronger disorder takes place which originates in a drastic decrease of the average hopping constant. The number of localized states increases but few states close to the band center exhibit a localization length about to or greater than the lattice size. The extended nature of these latter states is attributed to the occurrence of short range correlations in the random hopping constants.

DOI: 10.1103/PhysRevE.72.031901 PACS number(s): 87.14.Ee, 71.38.Ht, 63.20.Pw, 63.22.+m

I. INTRODUCTION

In the 1970s, Davydov and co-workers [1,2] developed a soliton formalism to explain how the energy released by the hydrolysis of adenosine triphophate (ATP) can be transported in α-helices. The main idea is that the released energy is responsible for the excitation of the high-frequency amide-I vibration of a peptide group. The dipole-dipole coupling between the different peptide groups leads to the delocalization of the internal vibrations and to the formation of vibrons. However, the interaction between the vibrons and the phonons of the helix induces a nonlinear dynamics which yields the creation of the so-called Davydov soliton (for a recent review, see for instance Refs. [3,4]).

Although this formalism gives a comprehensive schema which explains energy transport in living systems, there is no clear evidence of the existence of solitons in real proteins. Therefore, it has been suggested by Brown and co-workers [5,6] and by Ivic and co-workers [7–9] that the solution to the Davydov problem is rather a small polaron than a soliton. In fact, the soliton provides an approximate solution to the Davydov problem when the vibron bandwidth is greater than the phonon cutoff frequency, i.e., within the adiabatic limit. However, as mentioned by these authors, the situation is very different in proteins since the vibron bandwidth is lower than the phonon cutoff frequency. As a consequence, the quantum behavior of the phonons plays a crucial role and the nonadiabatic limit is reached. The creation of a vibron induces a virtual cloud of phonons describing a localized lattice distortion which accompanies the vibron. The vibron dressed by the lattice distortion forms the small polaron. Note that, recently, the femtosecond pump-probe spectroscopy of the N-H mode in a stable α-helix [10,11] has been successfully interpreted within an improved small polaron formalism [12,13]. Vibrational self-trapping in helices was thus observed for the first time, validating in the same time the small polaron approach.

Most of the theories applied to the Davydov problem involve a simple one-dimensional (1D) approximation of the real helix structure. Indeed, starting from a sequence of amino acid residues regularly distributed along a polypeptide chain, the helical 3D conformation is stabilized by the hydrogen bond between the carboxyl oxygen (CO) of an amino acid and the amide hydrogen (NH) of a second amino acid that is situated four residues ahead in the linear sequence. The helix is thus formed by three spines of hydrogen-bonded peptide units connected through covalent bonds [14]. Within the standard 1D Davydov model, the vibron-phonon dynamics of the helix is reduced to that of a single spine containing a set of identical amino acid residues. Therefore, the fundamental question arises whether the real helix structure affects the small polaron dynamics. The answer to this question requires the knowledge of too many parameters and appears as an intractable task due to the complex nature of the living world. We think that the Davydov model has to be improved step by step by adding successively relevant ingredients in order to reach a more realistic description of the vibron-phonon dynamics in proteins.

In that context, the influence of the 3D nature of a real α-helix has been studied within the soliton formalism (see for instance Refs. [15–17]) and more recently within the small polaron approach [18]. In the present paper, we focus our attention on a different aspect concerning the fact that an α-helix is built from a well-defined sequence of amino acids. All proteins in all species, from bacteria to humans, are formed from the same set of 20 amino acids. Each amino acid is characterized by its side chain which represents a particular molecular group. These 20 kinds of side chain vary in mass, shape, charge, hydrogen-bonding capacity, and

*Electronic address: vincent.pouthier@univ-fcomte.fr

chemical activities so that a given sequence of amino acids specifies the 3D protein conformation. Therefore, although the amino acid units are regularly distributed along the helix backbone, the protein exhibits a kind of random character due to the inhomogeneous mass distribution of the residues. This random character is assumed to strongly modify the external dynamics of the residues leading to a dramatic change in the nature of the phonons. Since the phonons participate in the dressing mechanism responsible for the polaron formation, the inhomogeneous mass distribution is expected to affect the vibron dynamics.

The aim of the present paper is to give a comprehensive theory to describe the influence of the inhomogeneous mass distribution in the amino acid sequence on the small polaron dynamics. Here, we restrict our attention to the single-polaron dynamics and we introduce a theory within the standard 1D Davydov model. The generalization to a 3D α-helix structure as well as to two-polaron dynamics will be addressed in forthcoming papers.

The influence of this inhomogeneity have been already studied by Förner and co-workers within the soliton formalism (see for instance Refs. [19–21]). To test the stability of the Davydov soliton against disorder, they assumed that the mass of each residue is a random variable uniformly distributed between the mass of the lightest amino acid (glycine) and the mass of the heaviest amino acid (tryptophane). Within the so-called D_2 *Ansatz* [19,20], they have shown that a soliton exists for amide-I vibrations and that the inhomogeneity does not affect significantly the formation and the motion of this soliton. Since no change accompanies the soliton dynamics, they concluded that an average-mass approximation is justified. Förner has also tested other *Ansätze* such as the so-called D_1 *Ansatz* [21] and the partial dressing model introduced by Brown and Ivic [5], which account for the quantum nature of the phonons. He has shown that no soliton occurs for the set of parameters describing the amide-I vibrations. More precisely, traveling solitons occur at a much larger threshold of the vibron-phonon coupling strength within the D_1 *Ansatz* and these solitons survive the mass disorder. By contrast, solitons were not found at all with the partial dressing model. Only dispersive solitary waves which are destroyed by the mass disorder, were obtained in this latter case.

The paper is organized as follows. The model to describe the vibron-phonon dynamics in a random α-helix is introduced in Sec. II. In Sec. III, the nature of the phonons is first summarized. Then, a modified Lang-Firsov transformation is applied to renormalize the vibron-phonon interaction and to reach the small polaron point of view [22]. Finally, a mean field procedure is used to obtain the effective polaron Hamiltonian. In Sec. IV, a numerical analysis of the properties of this Hamiltonian is given and the results are interpreted and discussed in Sec. V.

II. MODEL HAMILTONIAN

Within the standard model of Davydov, the vibron-phonon dynamics of an α-helix is reduced to the case of a single spine of hydrogen-bonded peptide units. Therefore, for a particular sequence, the amino acid residues are regularly distributed along a one-dimensional lattice formed by N sites. The nth site contains a amide-I vibration which behaves as a high frequency oscillator described by the standard creation and annihilation vibron operators b_n^+ and b_n. The vibron Hamiltonian is thus written as

$$H_v = \sum_n \hbar(\omega_0 - 2A) b_n^\dagger b_n - \sum_n \hbar J_1 (b_n^\dagger b_{n+1} + \text{H.c.}) \qquad (1)$$

where H.c. stands for the Hermitian conjugate, and ω_0 and A are the internal frequency and the anharmonic parameter of each amide-I mode, respectively. In Eq. (1), J_1 represents the lateral hopping constant between nearest neighbor residues. Note that the intramolecular anharmonicity has been implicitly taken into account according to the work detailed in Ref. [12] so that $J_1 = (1 + 0.93A/\omega_0)J$, where J is the corresponding harmonic hopping constant.

The amide-I vibrations interact with the phonons of the lattice which characterize the collective dynamics of the external motions of the residues. Within the harmonic approximation, the nth residue, with mass M_n, is assumed to perform a small displacement u_n around its equilibrium position and to interact with its neighboring residues via the force constant tensor $\mathbf{\Phi}$. The phonon Hamiltonian is thus written as

$$H_p = \sum_n \frac{p_n^2}{2M_n} + \frac{1}{2}\sum_{n,n'} \Phi(nn') u_n u_{n'} \qquad (2)$$

where p_n is the momentum associated with the displacement u_n. In an infinite lattice, the tensor $\mathbf{\Phi}$ is defined in terms of the force constant W between nearest neighbors as

$$\Phi(nn') = 2W\delta_{n,n'} - W\delta_{n,n'+1} - W\delta_{n,n'-1}.$$

The Davydov model suggests that the vibron-phonon interaction originates in the modulation of the vibrational frequency of each amide-I vibration by the external motion of the residues. The resulting coupling Hamiltonian is expressed as

$$\Delta H_{vp} = (1 + 2\eta)\sum_{n,n'} \chi \gamma_{nn'} u_{n'} b_n^\dagger b_n \qquad (3)$$

where $\eta = 6A/\omega_0$ denotes a correction to the harmonic approximation [12] and χ characterizes the strength of the vibron-phonon coupling. The matrix element $\gamma_{nn'}$ accounts for the perturbation of the nth amide-I vibration due to the motion of the n'th residue. In an infinite lattice, it is expressed as $\gamma_{nn'} = \delta_{n',n+1} - \delta_{n',n-1}$. Note that in the following section the numerical calculations will be performed by considering a finite size lattice. In this case, both the force constant tensor $\mathbf{\Phi}$ and the γ matrix have to be modified according to the theory detailed in Ref. [23].

In α-helices, the vibron-phonon interaction is assumed to be strong so that the vibron dynamics is essentially governed by the so-called dressing effect. The characterization of this effect requires the knowledge of both the phonon eigenstates and the Lang-Firsov transformation [22] which are introduced in the following section.

III. THEORETICAL BACKGROUND

A. Phonons in a random model of an α-helix protein

Due to the inhomogeneous nature of the amino acid sequence, the translational invariance of the phonon Hamiltonian is broken. Consequently, its diagonalization is not straightforward and numerical calculations are required to compute both the phonon eigenstates and eigenfrequencies. Nevertheless, before preforming such a numerical task, it is necessary to change slightly the formulation described in the previous section to define the phonon normal modes and to introduce the standard phonon creation and annihilation operators.

To proceed, let us define the reduced displacement of the nth residue as $v_n = u_n/\sqrt{M_n}$. In that case, the phonon Hamiltonian is rewritten as

$$H_p = \sum_n \frac{P_n^2}{2} + \frac{1}{2}\sum_{n,n'} D(nn')v_n v_{n'} \tag{4}$$

where P_n is the momentum associated to the displacement v_n and where $\boldsymbol{D}$ stands for the dynamical matrix defined in terms of the force constant tensor $\boldsymbol{\Phi}$ and of the diagonal mass matrix $\boldsymbol{M}$ as

$$\boldsymbol{D} = \boldsymbol{M}^{-1/2}\boldsymbol{\Phi}\boldsymbol{M}^{-1/2}. \tag{5}$$

At this step, the normal mode decomposition is achieved by performing the diagonalization of the dynamical matrix $\boldsymbol{D}$. Such a procedure allows us to define N eigenvalues Ω_λ^2 and N eigenvectors $\xi_\lambda(n)$ labeled by the index $\lambda = 1, 2, \ldots, N$. The index λ refers to a particular phonon mode with energy $\hbar\Omega_\lambda$ and for which the quantum dynamics is described by the well-known creation $a_\lambda^\dagger$ and annihilation a_λ operators. The phonon Hamiltonian is finally rewritten in the standard form as

$$H_p = \sum_\lambda \hbar\Omega_\lambda (a_\lambda^\dagger a_\lambda + 1/2) \tag{6}$$

whereas the displacement of the nth residue is expressed as

$$u_n = \sum_\lambda \sqrt{\frac{\hbar}{2M_n\Omega_\lambda}}(a_\lambda^\dagger + a_\lambda)\xi_\lambda(n). \tag{7}$$

Finally, the vibron-phonon coupling Hamiltonian Eq. (3) can be rewritten in terms of the phonon normal modes as

$$\Delta H_{vp} = \sum_{\lambda n} \hbar\Delta_\lambda(n)(a_\lambda^\dagger + a_\lambda)b_n^\dagger b_n \tag{8}$$

where $\Delta_\lambda(n)$ accounts for the modulation of the frequency of the nth amide-I vibration due to its coupling with the λth phonon mode. It is defined as

$$\Delta_\lambda(n) = (1+2\eta)\sum_{n'} \chi\gamma_{nn'}\sqrt{\frac{1}{2\hbar\Omega_\lambda M_{n'}}}\xi_\lambda(n'). \tag{9}$$

Note that a zero frequency eigenstate occurs in the phonon spectrum, whatever the size of the lattice. This state describes a uniform translation which does not modify the chemical surrounding of each amide-I vibration. As a result, it is not coupled with the vibrons and will be disregarded in the following of the text.

Due to the inhomogeneity of the amino acid sequence, the dynamical matrix is equivalent to that of a disordered chain in which the randomness strongly affects the nature of the phonons (see for instance [26–28]). Indeed, since the seminal paper of Anderson [29], it is well known that all the eigenstates of a 1D tight binding problem are exponentially localized in the asymptotic sense even if the disorder is infinitesimally small (see for a recent review Ref. [30]). Because the collective dynamics of a disordered chain can be mapped onto a tight binding model, most of the phonon normal modes are localized. However, in a finite size lattice, it has been shown that the chain supports a few delocalized low-frequency modes whose the number is about $\sqrt{N}$ [31–33].

As a consequence, Eqs. (8) and (9) clearly show that the vibrons will be affected by the inhomogeneous nature of the amino acid sequence through their coupling with the phonon normal modes. This coupling depends on both the eigenvalues and the eigenvectors of the random dynamical matrix. In particular, the localized nature of the phonon normal modes is responsible for a strong n dependence of the vibron-phonon coupling $\Delta_\lambda(n)$ in marked contrast with the simple phase dependence which occurs in the standard Davydov model.

B. Small polaron theory and effective Hamiltonian

To partially remove the vibron-phonon coupling Hamiltonian, a Lang-Firsov transformation is applied [12,22]. Indeed, since the vibron-phonon dynamics is dominated by the dressing effect, we consider a "full dressing" and introduce the following unitary transformation:

$$U = \exp\left(\sum_{\lambda n}^{*} \frac{\Delta_\lambda(n)}{\Omega_\lambda}(a_\lambda^\dagger - a_\lambda)b_n^\dagger b_n\right) \tag{10}$$

where the symbol $*$ in the sum means that the zero frequency phonon mode is excluded. By using Eq. (10), the transformed Hamiltonian $\hat{H} = U(H_v + H_p + \Delta H_{vp})U^\dagger$ is written as

$$\hat{H} = \sum_n \hbar[(\omega_0 - 2A)b_n^\dagger b_n - E_B(n)b_n^\dagger b_n - J_1(\Theta_n^\dagger\Theta_{n+1}b_n^\dagger b_{n+1} + \text{H.c.})] + \sum_\lambda \hbar\Omega_\lambda(a_\lambda^\dagger a_\lambda + 1/2) \tag{11}$$

where Θ_n denotes the local dressing operator defined as

$$\Theta_n = \exp\left(-\sum_{\lambda n}^{*} \frac{\Delta_\lambda(n)}{\Omega_\lambda}(a_\lambda^\dagger - a_\lambda)\right) \tag{12}$$

and where $E_B(n)$ is the local small polaron binding energy defined as

$$E_B(n) = \hbar\sum_\lambda^{*} \frac{|\Delta_\lambda(n)|^2}{\Omega_\lambda}. \tag{13}$$

In this dressed vibron point of view [Eq. (11)], the vibron-phonon coupling remains through the modulation of the lateral terms by the dressing operators. Although these opera-

tors depend on the phonon coordinates in a highly nonlinear way, the vibron-phonon interaction has been strongly reduced by this transformation. As a result, we can take advantage of such a reduction to perform a mean field procedure [7,8] and to express the full Hamiltonian $\hat{H}$ as the sum of three separated contributions as

$$\hat{H} = H_{eff} + H_p + \Delta H \tag{14}$$

where $H_{eff}=\langle(\hat{H}-H_p)\rangle$ denotes the effective Hamiltonian of the dressed vibrons and where $\Delta H=\hat{H}-H_p-\langle(\hat{H}-H_p)\rangle$ stands for the remaining part of the vibron-phonon interaction. The symbol $\langle\cdots\rangle$ represents a thermal average over the phonon degrees of freedom which are assumed to be in thermal equilibrium at temperature T.

Then, the effective dressed vibron Hamiltonian is written as

$$H_{eff} = \sum_n \hbar\hat{\omega}_0(n) b_n^\dagger b_n - \hbar J(n)(b_n^\dagger b_{n+1} + \text{H.c.}) \tag{15}$$

where $\hat{\omega}_0(n)=\omega_0-2A-E_B(n)/\hbar$ and where $J(n)=J_1\langle\Theta_n^\dagger\Theta_{n+1}\rangle$ denotes the thermal average of the product of the dressing operators involved in the polaron hop between the sites n and $n+1$.

At this step, the Hamiltonian H_{eff} describes the dynamics of vibrons dressed by a virtual cloud of phonons, i.e., small polarons. It takes into account the renormalization of the main part of the vibron-phonon coupling within the nonadiabatic limit. The interaction Hamiltonian ΔH, which characterizes the coupling between these dressed vibrons and the remaining phonons, is responsible for phase relaxation. It is assumed to be small in order to be treated by using perturbation theory and will be addressed in a forthcoming paper.

When compared with the standard polaron formalism, Eq. (15) clearly shows that the local nature of the vibron-phonon coupling $\Delta_\lambda(n)$ strongly modifies the polaron Hamiltonian. Indeed, both the frequency $\hat{\omega}_0(n)$ and the hopping constants $J(n)$ behave as n-dependent variables which exhibit a random nature through the randomness of the phonon normal modes which participate in the dressing mechanism. As a consequence, it is straightforward to show that the Schrodinger equation connected to single polaron states reduces to a 1D tight binding model with *a priori* both diagonal and off-diagonal disorder. Nevertheless, as shown in Appendix A, the small polaron binding energy $E_B(n)$ defined in Eq. (13) appears site independent and is equal to the value occurring in the standard Davydov model, i.e., $E_B=[(1+2\eta)\chi]^2/W$. This result originates in the fact that the Lang-Firsov transformation is responsible for a translation of the phonon field proportional to the vibron population. Such a translation does not modify the phonon kinetic energy but affects the phonon potential energy, only. As a result, the renormalization of the vibron frequency is insensitive to the mass of the residues.

Finally, due to the inhomogeneous nature of the amino acid sequence, the small polaron dynamics is described by a 1D tight binding model with off-diagonal disorder, only. The random nature of the hopping constants $J(n)$ is related to the random distribution of the residues through the dressing mechanism. This disorder, expected to favor the occurrence of localized states, is described in the following section.

TABLE I. Amino acids used to generate the random sequences of the residues.

Amino acid	Abbreviation	Mass (dalton)
Alanine	Ala	15.04
Glutamic acid	Glu	72.07
Leucine	Leu	57.13
Methionine	Met	75.16
Lysine	Lys	73.16
Arginine	Arg	101.18
Histidine	His	81.11
Valine	Val	43.10

IV. NUMERICAL RESULTS

In this section, a numerical analysis of the effective Hamiltonian Eq. (15) is performed with a special attention to the influence of the amino acid sequence on the behavior of the hopping constants $J(n)$. To proceed, the quantum energy for an amide-I vibration is fixed to $\omega_0=1665\ \text{cm}^{-1}$ and the well admitted value for the hopping constant $J=7.8\ \text{cm}^{-1}$ is used (see for instance Refs. [3,8]). From both recent calculations and experiments, the anharmonic constant of the amide-I vibration is equal to $A=8.0\ \text{cm}^{-1}$ [12,24,25] so that $J_1\approx J$ and $\eta=2.88\times10^{-2}$. The phonon force constant W, expected to range between 13 and 19.5 N m^{-1}, is fixed to $W=15\ \text{N m}^{-1}$. Finally, the strength of the vibron-phonon coupling will be considered as a free parameter allowed to vary around the standard value $\chi=62$ pN.

To determine the mass of the residues let us remind that along a single spine of hydrogen-bonded peptide units each amino acid residue is formed by a C═O group and a N—H group and involves a side chain and an hydrogen atom linked to an α-carbon. Therefore, the mass of the nth residue can be expressed as $M_n=M_0+M_{R_n}$ where $M_0=9.30\times10^{-26}$ kg denotes a reference mass whereas M_{R_n} stands for the mass of the nth side chain. To simulate the inhomogeneous nature of the sequence of the residues, we thus consider a random distribution involving the eight amino acids listed in Table I, only. In that context, each site of the lattice can be occupied by one of these eight residues with a probability equal to 1/8. Indeed, it is well known that among the 20 amino acids, only a few of them favor the occurrence of an helical conformation of the protein. For instance, alanine, glutamic acid, leucine, and methionine allow for the formation of helices whereas proline, glycine, tyrosine, and serine prevent such a three-dimensional conformation [14].

The behavior of the hopping constants $J(n)$ for a particular amino acid sequence is illustrated in Fig. 1 for $T=50$ (open circles), 150 (open squares), and 300 K (open triangles). In each case, the hopping constants exhibit random fluctuations around an average value which decreases as both

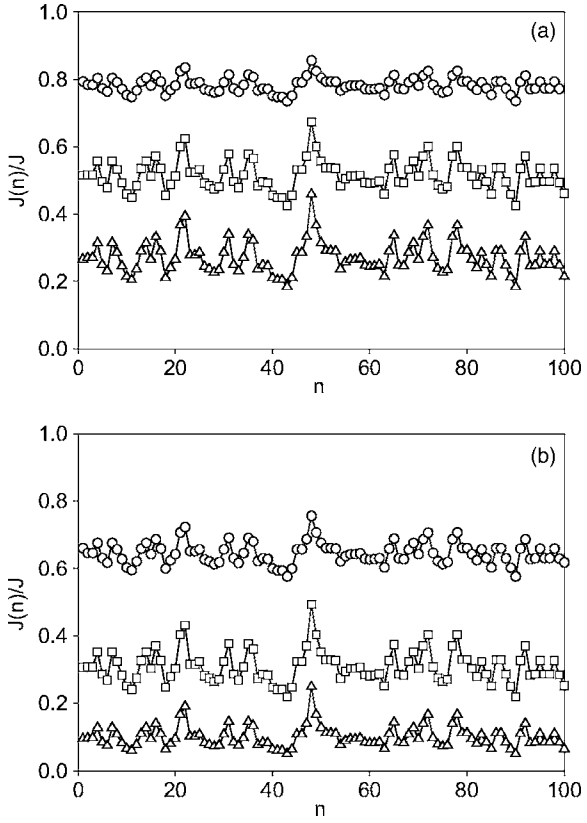

FIG. 1. Polaron hopping constants $J(n)$ vs the bond index n for a given sequence of amino acid residues. The parameters are $N=100$, $J=7.8$ cm^{-1}, $W=15$ N m^{-1}, $\chi=$(a) 60, and (b) 80 pN. Three temperatures have been considered, i.e., $T=50$ (open circles), 150 (open squares), and 300 K (open triangles).

T and χ increase. When $\chi=60$ pN [Fig. 1(a)], the fluctuations are rather small at low temperature ($T=50$ K) and $J(n)/J$ ranges between 0.73 and 0.85. As when T increases, the amplitude of these fluctuations increases and $J(n)/J$ ranges between 0.42 and 0.67 when $T=150$ K whereas it varies between 0.18 and 0.45 when $T=300$ K. In the same way, when $\chi=80$ pN [Fig. 1(b)], the fluctuations are rather small at low temperature ($T=50$ K) and increases when $T=150$ K. However, in marked contrast with the previous situation, the fluctuations slightly decrease when the temperature reaches $T=300$ K. For instance, $J(n)/J$ ranges between 0.21 and 0.49 when $T=150$ K whereas it varies between 0.05 and 0.25 when $T=300$ K.

In Fig. 2, the effective hopping constant $J_{eff}=\overline{J(n)}$ defined as the average hopping constant over the disordered amino acid sequence is displayed versus the temperature for $\chi=60$ (open circles), 70 (open squares), and 80 pN (open triangles). The lattice size is fixed to $N=200$. The figure corroborates the previous results and shows, in agreement with the standard dressing theory, that the effective hopping constant decreases as both T and χ increase. For instance, at $T=10$ K, the average hopping constant is equal to 6.87 and 6.21 cm^{-1} when χ is equal to 60 and 80 pN, respectively. In the same way, at $T=300$ K, the average hopping constant ranges between 2.10 and 1.32 cm^{-1} when χ varies from 60 to 80 pN, respectively. Note that the full lines correspond

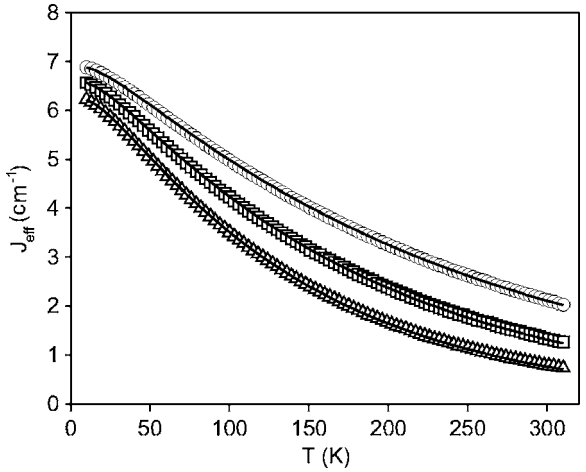

FIG. 2. Average hopping constant vs temperature for $\chi=60$ (open circles), 70 (open squares), and 80 pN (open triangles). The parameters are $N=200$, $J=7.8$ cm^{-1}, $W=15$ N m^{-1}. The full lines represent the hopping constant within the standard Davydov model in which the mass of the residues is fixed to the average mass (see the text).

to the effective hopping constant of an ordered lattice characterized by identical residues which the mass is fixed to the average mass of the eight amino acids considered in the simulation. It is shown that this latter effective hopping constant is almost equal to the average hopping constant. This feature reveals that the random amino acid sequence generates rather small fluctuations in the polaron Hamiltonian.

The behavior of the fluctuations of the polaron hopping constants is shown in Figs. 3–5 via the analysis of the correlation function $C(\delta)=\Delta J(n)\Delta J(n+\delta)$ where $\Delta J(n)=J(n)-J_{eff}$. The evolution of the correlation function $C(0)$ versus the temperature is displayed in Fig. 3 for $N=200$. Whatever the strength of the vibron-phonon coupling χ, the behavior of the correlation function is characterized by a critical tem-

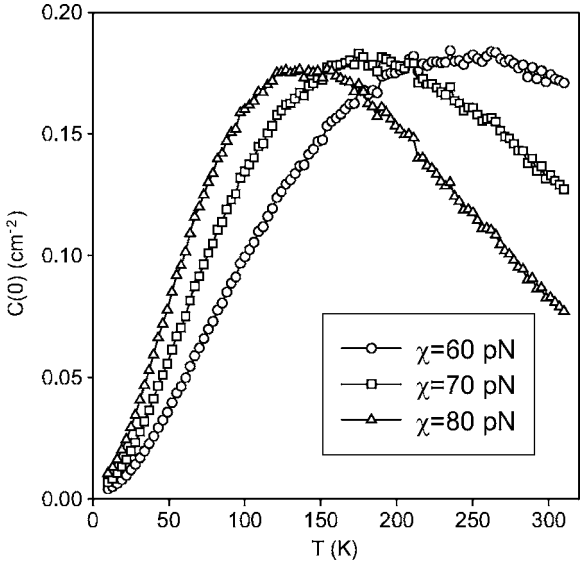

FIG. 3. Correlation function of the hopping constant $C(0)$ vs temperature for $N=200$, $J=7.8$ cm^{-1}, and $W=15$ N m^{-1}.

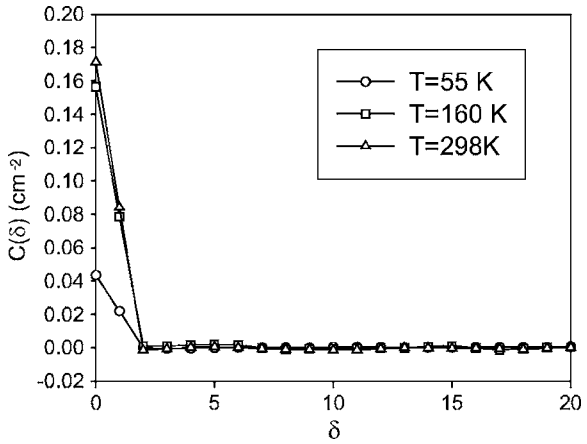

FIG. 4. Correlation function of the hopping constant $C(\delta)$ vs δ for $N=200$, $J=7.8$ cm^{-1}, $W=15$ N m^{-1}, and $\chi=60$ pN; $T=55$ (open circles), 160 (open squares), and 298 K (open triangles).

perature T_c which discriminates between two regimes. When $T<T_c$, the correlation $C(0)$ increases as the temperature increases to reach a maximum value when $T=T_c$. By contrast, when $T>T_c$, the correlation function decreases in an almost linear way as the temperature increases. The maximum value of $C(0)$ appears almost independent on the vibron-phonon coupling strength and lies below 0.20 cm^{-2}. In agreement with the features observed in Fig. 2, this small value indicates that the random character of polaron Hamiltonian is rather weak. As shown in Fig. 3, the critical temperature strongly depends on the χ value and it decreases as χ increases. For instance, the critical temperature is located around 250 K when $\chi=60$ pN whereas it occurs around 125 K when $\chi=80$ pN. Note that since $C(0)$ is a measure of the fluctuations of the hopping constants, these features corroborate the results displayed in Fig. 1.

In Fig. 4, the behavior of the correlation function $C(\delta)$ with the distance δ is shown for $N=200$ and $\chi=60$ pN. Whatever the temperature, the figure reveals that the random polaron Hamiltonian is characterized by a correlated disorder. Nevertheless, the disorder exhibits short range correlations only since $C(\delta)$ almost vanishes when $\delta \geqslant 2$. In other words, the correlation function takes significant values for $\delta=0$ and $\delta=1$, only, and the figure clearly shows that $C(0) \approx 2C(1)$. The temperature modifies the amplitude of the correlation function according to the results shown in Fig. 3 but does not affect the range of the correlation function. Note that the same features are observed in Fig. 5 where the behavior of $C(\delta)$ is displayed for $N=200$ and $T=298$ K for various χ values. Indeed, whatever the strength of the vibron-phonon coupling, the disordered nature of the polaron Hamiltonian is characterized by short range correlations and, as previously, $C(\delta)$ almost vanishes when $\delta \geqslant 2$.

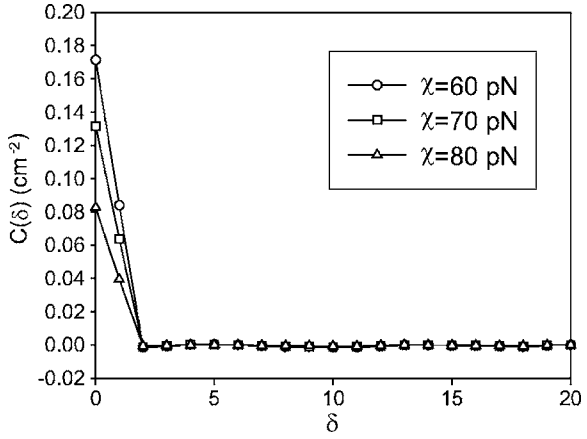

FIG. 5. Correlation function of the effective hopping constant $C(\delta)$ vs δ for $N=200$, $J=7.8$ cm^{-1}, $W=15$ N m^{-1}, and $T=298$ K; $\chi=60$ (open circles), 70 (open squares), and 80 pN (open triangles).

From the standard localization theory, it is well known that the main consequence of the random nature of the polaron Hamiltonian is the occurrence of localized states. As discussed in numerous papers (see for instance Refs. [30,34,35]), a way to discriminate between localized and extended states is based on the analysis of the corresponding inverse participation ratio. In terms of the αth small polaron wave function $\psi_\alpha(n)$, the inverse participation ratio $P(\omega_\alpha)^{-1}$ is defined as

$$P(\omega_\alpha)^{-1} = \sum_n |\psi_\alpha(n)|^4 \tag{16}$$

where ω_α denotes the eigenenergy of the αth polaron state. In that context, for an ordered finite size lattice containing N sites, the polaron wave functions correspond to extended stationary states characterized by an inverse participation ratio $P(\omega_\alpha)^{-1}=1.5/(N+1)$. In the opposite situation associated to a state strongly localized onto a single site, the inverse participation ratio is equal to unity. Therefore, to discriminate between localized and extended states, we introduced the normalized participation ratio $1.5P(\omega_\alpha)/(N+1)$ which ranges between unity (extended states) and $1.5/(N+1)$ (strongly localized states).

The behavior of the normalized participation ratio is illustrated in Fig. 6 for $N=200$, $T=10$ (open circles), 150 (open squares), and 300 K (open triangles). In Fig. 6(a), the vibron-phonon coupling strength is fixed to $\chi=60$ pN whereas it is equal to $\chi=80$ pN in Fig. 6(b). Note that no average has been performed so that the normalized participation ratio corresponding to several random configurations has been reported on the figures.

Figure 6(a) clearly shows that the finite size polaron Hamiltonian supports both extended and localized states lying in a band centered around $\omega_0-2A-E_B/\hbar$ (which has been used as the reference) over a frequency range of about $2J_{eff}$. However, the temperature strongly affects the nature of these states. First, due to the dressing effect, the bandwidth depends on the temperature and it decreases as the temperature increases. Then, the localized or extended nature of the states depends on the temperature. At low temperature, most of the states lying in the core of the band appear extended and are rather insensitive to the disorder. By contrast, the states located in the vicinity of the band edges experience strong modifications and appear drastically localized in a perfect agreement with the weak disorder theory. This feature is reinforced when the temperature is increased. More pre-

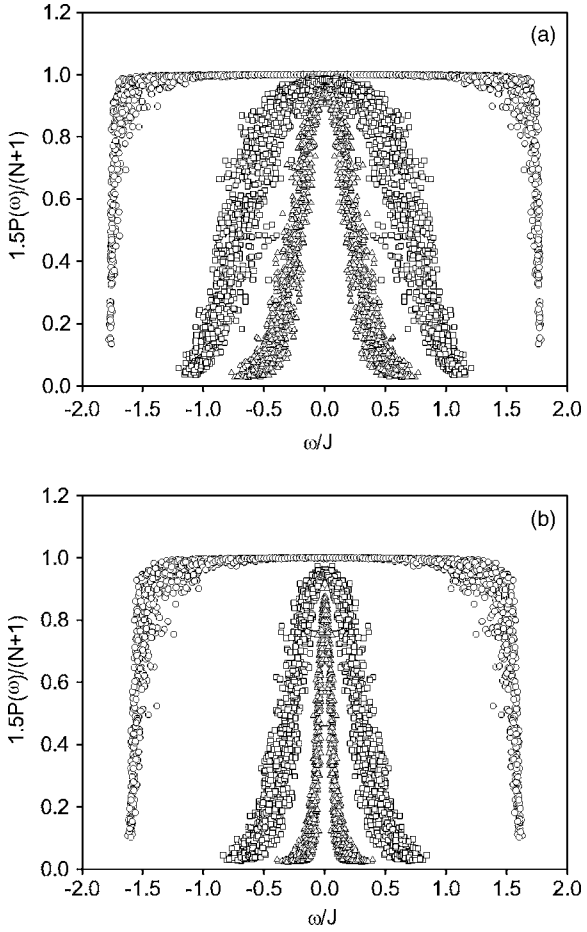

FIG. 6. Normalized participation ratio vs energy for $N=200$, $J=7.8$ cm^{-1}, $W=15$ N m^{-1}, $T=10$ (open circles), 150 (open squares), and 300 K (open triangles) and for $\chi=$(a) 60 and (b) 80 pN.

cisely, at higher temperature, the number of localized states increases. They remain in the tails of the normalized participation ratio which takes place close to the band edges and which the width increases with the temperature. Nevertheless, the normalized participation ratio is always maximum at the center of the band indicating that the states located around the band center exhibit an extended nature. In other words, these latter states are characterized by a localization length about to or greater than the lattice size.

The same features are observed in Fig. 6(b) when $\chi=80$ pN. However, the figure clearly shows that at low temperature, the normalized participation ratio appears slightly modified by an increase of the vibron-phonon coupling strength. This is no longer the case at higher temperature where an increase of χ reinforces the localization mechanism induced by the temperature.

This latter effect is illustrated in Fig. 7 where the temperature dependence of the normalized participation ratio at the frequency equal to $0.25J$ is displayed for $N=200$. The figure clearly shows the occurrence of a transition which discriminates between an extended and a localized nature of the states with an energy equal to $0.25J$. Indeed, when $T<50$ K, the normalized participation ratio is close to unity and appears almost independent on the vibron-phonon coupling strength. In other words, whatever the strength of the

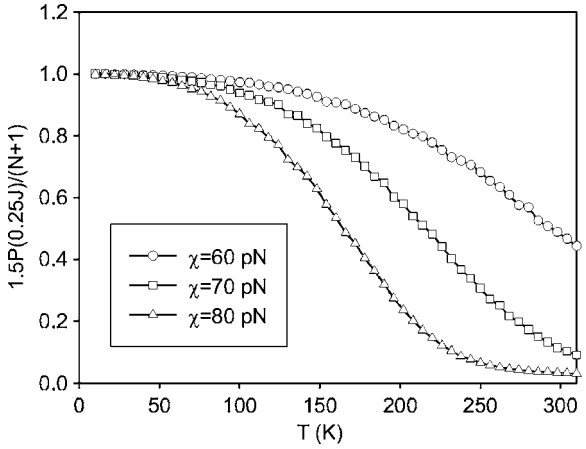

FIG. 7. Normalized participation ratio at $\omega=0.25J$ vs T for $N=200$, $J=7.8$ cm^{-1}, $W=15$ N m^{-1}, $\chi=60$ (open circles), 70 (open squares), and 80 pN (open triangles).

vibron-phonon coupling, the corresponding states are fully delocalized over the whole lattice at low temperature. In marked contrast, when $T>50$ K, the normalized participation ratio strongly depends on the vibron-phonon coupling strength. For a small χ value, i.e., $\chi=60$ pN, the normalized participation ratio slightly decreases as the temperature increases to reach 0.49 at $T=298$ K. In that case, the corresponding states tend to slightly localize. Such a behavior is reinforced as when the coupling constant χ is increased. For instance, when $\chi=80$ pN, the normalized participation ratio rapidly decreases as T increases to reach an almost constant value equal to 0.03 when $T>260$ K. In other words, an increase of the vibron-phonon coupling enhances the localization process so that the corresponding states become strongly localized.

Finally, to illustrate the difference between extended and localized states, the modulus square of three polaron wave functions for $N=200$, $T=300$ K, and $\chi=60$ pN are reported in Fig. 8. The corresponding energies are (a) $-0.4966J$, (b) $0.0078J$, and (c) $0.4022J$. Figure 8 clearly shows that both

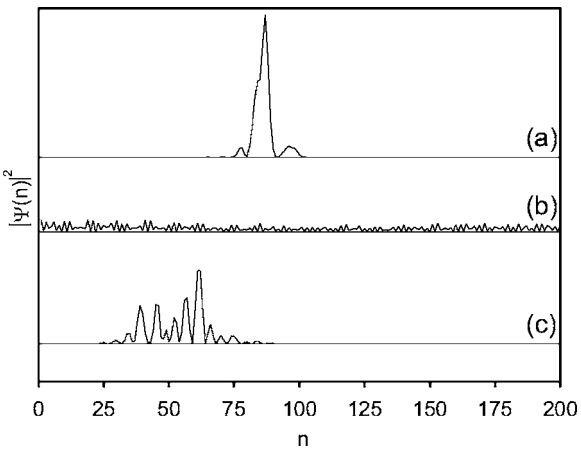

FIG. 8. Modulus squared of three polaron wave functions for $N=200$, $J=7.8$ cm^{-1}, $W=15$ N m^{-1}, $T=300$ K, and $\chi=60$ pN. The corresponding energies are (a) $-0.4966J$ (b) $0.0078J$, and (c) $0.4022J$.

the low frequency and the high frequency states correspond to strongly localized wave functions. By contrast, the state for which the energy lies close to the band center extends over the whole lattice according to a standard stationary wave function.

V. DISCUSSION AND INTERPRETATION

To interpret the previous numerical results, let us first discuss the nature of the disorder which affects the small polaron dynamics. Such a disorder arises when a vibron is dressed by the phonons associated to the collective dynamics of the residues which belong to the inhomogeneous amino acid sequence of the helix. The inhomogeneity in the mass distribution of the residues yields a rather strong disorder which drastically modifies the phonon dynamics. Indeed, as listed in Table I, the sequence we have considered involves a random distribution of eight amino acids which cover a wide range of distinct masses. For instance, the mass of the side chain of alanine is equal to 15.04 dalton whereas the mass of the side chain of arginine, almost seven times greater, is equal to 101.18 dalton. In addition, the amino acid sequence is generated by assuming that the masses form a set of independent random variables. As a result, the disorder in the sequence does not exhibit any spatial correlation.

As shown in the previous section, the disorder which affects the small polaron dynamics is rather different from the disorder in the amino acid sequence, although this latter one is at the origin of the former one. More precisely, the small polaron dynamics is described by a 1D tight binding model with off-diagonal disorder, only. We have shown that the renormalized frequency of each amide-I mode does not experience any randomness so that the disorder occurs in the hopping constants $J(n)$ which form a set of random variables. These hopping constants exhibit rather small fluctuations around an average value which behaves like the effective hopping constant for an ordered lattice with identical residues with a mass equal to the average mass. Note that these features corroborate the results obtained by Förner and co-workers within the so-called D_2 *Ansatz* [19,20] and who have shown that the average-mass approximation is justified. However, they concluded that the inhomogeneities in the mass distribution do not affect the dynamics of the Davydov soliton whereas our results clearly show that they can strongly modify the polaron dynamics. Indeed, due to the dressing mechanism, the behavior of the hopping constants depends on both the temperature and the strength of the vibron-phonon coupling and two regimes occur which discriminate between a weak and a strong disorder. At low temperature, the hopping constants are characterized by small fluctuations around a rather large average value. In other words, the dressing mechanism induces a kind of softening of the randomness so that the polaron Hamiltonian appears weakly disordered. As when increasing the temperature a stronger disorder takes place although the hopping constant fluctuations remain rather small. In fact, the strength of the disorder does not originate in a drastic increase of the hopping constant fluctuations but is essentially due to the fact that the average hopping constant decreases as the temperature increases. As a result, the ratio between the amplitude of the fluctuations and the average hopping constant always increases with the temperature. In the same may, the disorder is enhanced by an increase of the vibron-phonon coupling. As previously, although the hopping constant fluctuations do not depend dramatically on this coupling strength, the average hopping constant is strongly reduced when the coupling strength is increased.

Our simulation has revealed the occurrence of a critical temperature which discriminates between two regimes for the fluctuations of the hopping constants. Below the critical temperature, the fluctuations increase with the temperature whereas the opposite feature takes place above the critical temperature. This behavior is attributed to the fact that the hopping constants form a set of positive random variables for which lower value of the distribution is bound by zero. As a result, at low temperature, the average hopping constant is sufficiently strong so that the distribution appears rather symmetric. It does not experience the boundary at the origin and its width increases with the temperature. However, when the critical temperature is reached, the average hopping constant is reduced so that the boundary at the origin tends to modify the shape of the distribution which becomes rather asymmetric. A narrowing effect of the distribution takes place so that the hopping constant fluctuations decrease as the temperature increases.

Finally, our results reveal that the polaron Hamiltonian is characterized by a correlated disorder since the hopping constants $J(n)$ do not form a set of independent variables. More precisely, short range correlations occur so that the hopping constant $J(n)$ is linked to the nearest neighbor hopping constants $J(n\pm1)$. As shown in Appendix B, these short range correlations originate in the mass dependence of the hopping constants. Indeed, the hopping constant $J(n)$ involves the masses of a reduced number of residues located around the sites n and $n+1$. For instance, at high temperature, $J(n)$ depends explicitly on the masses M_{n-1}, M_n, M_{n+1}, and M_{n+2}. As a result, the hopping constants $J(n\pm1)$ involve common masses with the hopping constant $J(n)$ so that short range correlations occur although the masses form a set of independent random variables.

The occurrence of both a short range correlated disorder and a transition between a weak and a strong disorder strongly modify the polaron wave functions. Indeed, the analysis of the normalized participation ratio has revealed that in the weak disorder limit, i.e., at low temperature, extended states occur over a wide range of energies around the band center. However, the states which the energy lies in the vicinity of the band edges are strongly affected by the disorder and appears localized. This feature was shown to be rather insensitive to the strength of the vibron-phonon coupling. By contrast, in the strong disorder limit, i.e. at high temperature, the number of localized states increases drastically and the localization process is enhanced by the vibron-phonon coupling. Nevertheless, the states in the vicinity of the band center appears slightly perturbed by the disorder and are characterized by a localization length greater than or about to the lattice size.

To understand these features, let us take advantage of the fact that the hopping constants perform small fluctuations

around their average value so that a second order perturbative theory can be applied. To proceed, we define the zero order polaron Hamiltonian as the average effective Hamiltonian as

$$H_0 = \sum_n \hbar\hat{\omega}_0 b_n^\dagger b_n - \hbar J_{eff}(b_n^\dagger b_{n+1} + \text{H.c.}) \tag{17}$$

where $J_{eff}=\overline{J(n)}$ is the average hopping constant introduced in the previous section. In an infinite lattice, the quantum states of H_0 are plane waves with wave vector q and eigenfrequencies $\omega_q=\hat{\omega}_0-2J_{eff}\cos(q)$ defining the polaron band. Note that the wave vector q lies in the first Brillouin zone of the lattice, i.e., $-\pi<q<\pi$. To recover the effective polaron Hamiltonian H_{eff} [Eq. (15)], a coupling Hamiltonian V has to be added to the reference Hamiltonian H_0. This coupling is defined as

$$V = \sum_n -\hbar\Delta J(n)(b_n^\dagger b_{n+1} + \text{H.c.}) \tag{18}$$

where $\Delta J(n)=J(n)-J_{eff}$. Within the standard second order theory, a measure of the perturbation induced by the coupling V onto the eigenstates of H_0 is given by the average relaxation rate $W(q)$. This rate, which characterizes the decay of the plane wave q over all the other plane waves is defined as

$$W(q) = 2\pi\sum_{q'} \overline{|\langle q'|V|q\rangle|^2}\,\delta(\omega_q - \omega_{q'}). \tag{19}$$

After performing straightforward algebraic calculations, this rate is finally expressed in terms of the correlation function $C(\delta)=\overline{\Delta J(n)\Delta J(n+\delta)}$ as

$$W(q) = \sum_\delta \frac{C(\delta)}{J_{eff}}\frac{1+\cos(2q)+2\cos(2q\delta)}{|\sin(q)|}. \tag{20}$$

From the knowledge of the relaxation rate, the spatial extension of the state with wave vector q can be characterized by introducing the localization length defined as $\xi_q=4|v_q|/W(q)$ where $v_q=2J_{eff}\sin(q)$ denotes the group velocity of the qth plane wave.

The behavior of the localization length vs the energy is illustrated in Fig. 9. Two situations have been considered. In the first situation (full circles in Fig. 9), the correlations in the disorder have been neglected so that it has been assumed that $C(\delta)$ vanishes when $\delta\neq 0$. In that case, the relaxation rate is defined as

$$W(q) = \frac{C(0)}{J_{eff}}\frac{3+\cos(2q)}{|\sin(q)|} \tag{21}$$

whereas the localization length is expressed as

$$\xi_q = \frac{8J_{eff}^2\sin^2(q)}{C(0)}\frac{1}{3+\cos(2q)}. \tag{22}$$

As shown in Fig. 9, the localization length vanishes at the band edges and is maximum at the band center. However, it remains finite over the entire polaron band which indicates that all the states are localized. Note that at the center of the band, the localization length is equal to $\xi_{\pi/2}=8J_{eff}^2\sin^2(q)/2C(0)$. This expression is equivalent to the localization length occurring in the 1D Anderson problem within the weak disorder limit and the factor $2C(0)$ plays the role of the standard deviation of the one-site random energies [30].

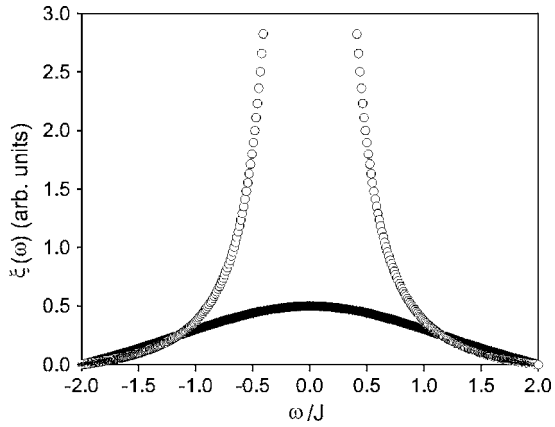

FIG. 9. Theoretical localization length for both uncorrelated (full circles) and correlated (open circles) disorder.

In fact, the interpretation of our numerical results requires to account for the correlations in the disorder. To proceed, we take advantage that the correlation function takes significant values for $\delta=0$ and $\delta=1$, only, according to the relation $C(0)\approx 2C(1)$. As a consequence, by considering these short range correlations the relaxation rate is defined as

$$W(q) = \frac{4C(0)}{J_{eff}}\frac{1+\cos(2q)}{|\sin(q)|} \tag{23}$$

whereas the localization length is expressed as

$$\xi_q = \frac{8J_{eff}^2\sin^2(q)}{C(0)}\frac{1}{4[1+\cos(2q)]}. \tag{24}$$

In that case, a remarkable feature occurs since Eq. (23) clearly shows that the relaxation rate vanishes when $q=\pi/2$. Therefore, although the localization length behaves almost like in the uncorrelated situation near the band edges, it drastically increases when the energy reaches the center of the band and explicitly diverges at the band center (see open circles in Fig. 9). In others words, short range correlations in the disorder do not significantly modify the localized nature of the states located close to band edges but they drastically enhance the delocalization of the states at the band center. These results are in perfect agreement with recent investigations which have revealed that 1D lattices can support extended states when the disorder exhibits spatial correlations. For instance, it has been shown within the so-called random

dimer model that short range correlations in on-site potentials can give rise to a discrete set of extended quantum states so that the corresponding localization length diverges only for discrete values of the energy [36–38]. Note that it has been shown that specific long-range correlations in potentials may lead to the emergence of a continuum of extended states (see for instance Ref. [39] and references therein).

Finally, as shown in Eq. (24), the strength of the localization length is proportional to $J_{eff}^2/C(0)$. Therefore, although the fluctuations of the hopping constants remains rather small, such a dependence indicates that the localization mechanism is governed by the behavior of the average hopping constant J_{eff}. According to the well-known dressing mechanism, we have shown that this effective constant is reduced by an increase of both the temperature and the vibron-phonon coupling strength. Such an increase results in an enhancement of the localization as observed in our numerical simulations.

VI. CONCLUSION

In this paper, a comprehensive theory was introduced to describe the influence of the inhomogeneous mass distribution in the amino acid sequence of an α-helix on the dynamics of amide-I vibrons. In α-helices, the vibrons are strongly coupled with the phonons associated to the external dynamics of the residues so that their dynamics is essentially governed by the so-called dressing effect. This effect favors the formation of small polarons which correspond to vibrons dressed by a virtual cloud of phonons. In that context, it has been shown that inhomogeneities in the amino acid sequence induce a randomness in the small polaron Hamiltonian through the dressing mechanism. The polaron dynamics is thus described according to a 1D tight binding model with correlated off-diagonal disorder, only. At low temperature, it has been shown that the hopping constants exhibit small fluctuations around a rather large average value so that the polaron Hamiltonian appears weakly disordered. Extended states occur over a wide range of energies around the band center whereas the states close to the band edges appear localized. By contrast, at biological temperature, a stronger disorder takes place which originates in a drastic decreases of the average hopping constant although the hopping constant fluctuations remain rather small. The number of strongly localized states increases but few states close to the band center remain slightly perturbed by the disorder and exhibit a localization length about to or greater than the lattice size. The extended behavior of these latter states was attributed to the existence of short range spatial correlations in the random hopping constants.

To conclude, let us mention that forthcoming works will be devoted to the study of the interaction of the polaron with the remaining phonons through the coupling Hamiltonian ΔH. This interaction will be responsible for an additional contribution to the relaxation rate and is expected to strongly modify the small polaron eigenstates. Therefore, it seems necessary to account about both the disorder and the coupling with the remaining phonons to address a complete theory to describe the transport properties in proteins.

ACKNOWLEDGMENT

The author would like to thank Dr. P. N. M. Hoang for fruitful discussions and for a critical reading of the text.

APPENDIX A: EXPRESSION OF THE SMALL POLARON BINDING ENERGY

From Eq. (13), the small polaron binding energy is expressed as

$$E_B(n) = \frac{[(1+2\eta)\chi]^2}{2} \sum_{\lambda,m,m'} \gamma_{nm}\gamma_{nm'} \frac{\xi_\lambda(m)}{\sqrt{M_m}} \frac{1}{\Omega_\lambda^2} \frac{\xi_\lambda(m')}{\sqrt{M_{m'}}}. \tag{A1}$$

From the definition of the dynamical matrix $\boldsymbol{D}$ Eq. (5), it is straightforward to show that the small polaron binding energy does not depend on the residue masses and is defined in terms of the force constant tensor $\boldsymbol{\Phi}$ as

$$E_B(n) = \frac{[(1+2\eta)\chi]^2}{2} \sum_{m,m'} \gamma_{nm}\gamma_{nm'}\Phi^{-1}(mm'). \tag{A2}$$

In an infinite lattice, the well-known Bloch transformation allows for the diagonalization of the force constant tensor. As a result, the small polaron binding energy is written as

$$E_B(n) = \frac{[(1+2\eta)\chi]^2}{2N} \sum_{m,m',k} \frac{\gamma_{nm}\gamma_{nm'}e^{ik(m-m')}}{2W[1-\cos(k)]}. \tag{A3}$$

By inserting the form of the corresponding γ matrix, Eq. (A3) is finally expressed as

$$E_B(n) = \frac{[(1+2\eta)\chi]^2}{N} \sum_{m,m',k} \frac{1+\cos k}{W} = \frac{[(1+2\eta)\chi]^2}{W}. \tag{A4}$$

APPENDIX B: CALCULATION OF THE HOPPING CONSTANT $J(n)$

From the definition of the dressing operators Eq. (12), the hopping constant $J(n)$ is expressed as

$$J(n) = J_1 \left\langle \exp\left(\sum_\lambda \frac{\Delta_\lambda(n) - \Delta_\lambda(n+1)}{\Omega_\lambda} (a_\lambda^\dagger - a_\lambda) \right) \right\rangle. \tag{B1}$$

After performing the average over the phonon degrees of freedom assumed to be in thermal equilibrium at the temperature T, the hopping constant $J(n)$ is written as

$$J(n) = J_1 \exp\left(-\sum_\lambda \left| \frac{\Delta_\lambda(n) - \Delta_\lambda(n+1)}{\Omega_\lambda} \right|^2 (n_\lambda + 1/2) \right) \tag{B2}$$

where $n_\lambda = 1/[\exp(\hbar\Omega_\lambda/k_BT) - 1]$ denotes the Bose distribution. By inserting the expression of $\Delta_\lambda(n)$ [Eq. (9)] in Eq. (B2), the hopping constant $J(n)$ becomes

$$J(n) = J_1 \exp\left(- \sum_{\lambda} \sum_{p,q} \frac{(1+2\eta)^2 \chi^2}{4\hbar} (\gamma_{n,p} - \gamma_{n+1,p})(\gamma_{n,q} - \gamma_{n+1,q}) \frac{\xi_\lambda(p)}{\sqrt{M_p}} \frac{1}{\Omega_\lambda^3} \coth \frac{\hbar \Omega_\lambda}{2k_B T} \frac{\xi_\lambda(q)}{\sqrt{M_q}} \right). \tag{B3}$$

To simplify the previous expression, let us introduce the local (4×4) matrix $\boldsymbol{A}_n$ in which the elements are defined as $A_n(p,q)=(\gamma_{n,p}-\gamma_{n+1,p})(\gamma_{n,q}-\gamma_{n+1,q})$. Therefore, it is straightforward to show that the hopping constant can be formally expressed as

$$J(n) = J_1 \exp\left\{ - \frac{(1+2\eta)^2 \chi^2}{4\hbar} \mathrm{Tr}\left[\boldsymbol{A}_n \boldsymbol{M}^{-1/2} \boldsymbol{D}^{-3/2} \coth\left(\frac{\hbar \boldsymbol{D}^{1/2}}{2k_B T} \right) \boldsymbol{M}^{-1/2} \right] \right\} \tag{B4}$$

At this step, Eq. (B4) yields the general expression of the hopping constant $J(n)$ which has been used for the numerical simulations presented in the text. It clearly shows that the mass dependence of the hopping constant is twofold. First, it arises directly via the occurrence of the mass matrices. Then, it is hidden in the definition of the random dynamical matrix. Nevertheless, at high temperature and for an infinite lattice, this expression can be simplified and it is straightforward to show that $J(n)$ is expressed as

$$J(n) = J_1 \exp\left(- \frac{(1+2\eta)^2 \chi^2 k_B T}{2\hbar} \mathrm{Tr}(\boldsymbol{B}_n \boldsymbol{\Phi}^{-2}) \right) \tag{B5}$$

where the mass dependence occurs in the (4×4) matrix $\boldsymbol{B}_n=\boldsymbol{M}^{1/2}\boldsymbol{A}_n\boldsymbol{M}^{1/2}$ defined in the subspace connected to the sites $n-1$, n, $n+1$, and $n+2$ as

$$\boldsymbol{B}_n = \begin{pmatrix} M_{n-1} & -\sqrt{M_{n-1}M_n} & -\sqrt{M_{n-1}M_{n+1}} & \sqrt{M_{n-1}M_{n+2}} \\ -\sqrt{M_nM_{n-1}} & M_n & \sqrt{M_nM_{n+1}} & -\sqrt{M_nM_{n+2}} \\ -\sqrt{M_{n+1}M_{n-1}} & \sqrt{M_{n+1}M_n} & M_{n+1} & -\sqrt{M_{n+1}M_{n+2}} \\ \sqrt{M_{n+2}M_{n-1}} & -\sqrt{M_{n+2}M_n} & -\sqrt{M_{n+2}M_{n+1}} & M_{n+2} \end{pmatrix}. \tag{B6}$$

[1] A. S. Davydov and N. I. Kisluka, Phys. Status Solidi B **59**, 465 (1973); Zh. Eksp. Teor. Fiz. **71**, 1090 (1976) [Sov. Phys. JETP **44**, 571 (1976)].

[2] A. S. Davydov, *Solitons in Molecular Systems* (D. Reidel, Dordrecht, 1985).

[3] A. C. Scott, Phys. Rep. **217**, 1 (1992).

[4] P. L. Christiansen and A. C. Scott, *Davydov's Soliton Revisited* (Plenum, New York, 1990).

[5] D. W. Brown and Z. Ivic, Phys. Rev. B **40**, 9876 (1989).

[6] D. W. Brown, K. Lindenberg, and X. Wang, in *Davydov's Soliton Revisited*, edited by P. L. Christiansen and A. C. Scott (Plenum, New York, 1990).

[7] Z. Ivic, D. Kapor, M. Skrinjar, and Z. Popovic, Phys. Rev. B **48**, 3721 (1993).

[8] Z. Ivic, D. Kostic, Z. Przulj, and D. Kapor, J. Phys.: Condens. Matter **9**, 413 (1997).

[9] J. Tekic, Z. Ivic, S. Zekovic, and Z. Przulj, Phys. Rev. E **60**, 821 (1999).

[10] J. Edler, R. Pfister, V. Pouthier, C. Falvo, and P. Hamm, Phys. Rev. Lett. **93**, 106405 (2004).

[11] J. Edler, V. Pouthier, C. Falvo, R. Pfister, and P. Hamm, in *Ultrafast Phenomena XIV*, edited by T. Kobayashi, T. Okada, T. Kobayashi, K. Nelson, S. De Silvesti, Springer Series in Chemical Physics Vol. 79 (Springer, Berlin, 2005).

[12] V. Pouthier, Phys. Rev. E **68**, 021909 (2003).

[13] V. Pouthier and C. Falvo, Phys. Rev. E **69**, 041906 (2004).

[14] L. Stryer, *Biochemistry*, 4th ed. (W. H. Freeman, New York, 1995).

[15] A. C. Scott, Phys. Rev. A **26**, 578 (1982).

[16] D. Hennig, Phys. Rev. B **65**, 174302 (2002).

[17] L. Brizhik, A. Eremko, B. Piette, and W. Zakrzewski, Phys. Rev. E **70**, 031914 (2004).

[18] C. Falvo and V. Pouthier, e-print physics/0502029.

[19] H. Motschmann, W. Förner, and J. Ladik, J. Phys.: Condens. Matter **1**, 5083 (1989).

[20] W. Förner and J. Ladik, in *Davydov's Soltion Revisited* (Ref. [4]).

[21] W. Förner, Phys. Rev. A **44**, 2694 (1991).

[22] I. G. Lang and Yu. A. Firsov, Sov. Phys. JETP **16**, 1293 (1962).

[23] C. Falvo and V. Pouthier, J. Chem. Phys. **122**, 014701 (2005).

[24] P. Hamm, M. Lim, and R. M. Hochstrasser, J. Phys. Chem. B **102**, 6123 (1998).

[25] S. Woutersen and P. Hamm, J. Phys.: Condens. Matter **14**, R1035 (2002).

[26] F. J. Dyson, Phys. Rev. **92**, 1331 (1953).

[27] H. Schmidt, Phys. Rev. **105**, 425 (1957).

[28] P. Dean, Rev. Mod. Phys. **44**, 127 (1972).

[29] P. W. Anderson, Phys. Rev. **109**, 1492 (1958).

[30] B. Kramer and A. MacKinnon, Rep. Prog. Phys. **56**, 1469 (1993).

[31] P. Dean, Proc. Phys. Soc. London **84**, 727 (1964).

[32] H. Matsuda and K. Ishii, Suppl. Prog. Theor. Phys. **45**, 56 (1970).

[33] K. Ishii, Suppl. Prog. Theor. Phys. **53**, 77 (1973).
[34] D. J. Thouless, Phys. Rep., Phys. Lett. **13**, 93 (1974).
[35] J. T. Edwards and D. J. Thouless, J. Phys. C **5**, 807 (1972).
[36] A. Bovier, J. Phys. A **25**, 1021 (1992).
[37] J. C. Flores, J. Phys.: Condens. Matter **1**, 8471 (1989).
[38] L. Tessier and F. M. Izrailev, Physica E (Amsterdam) **9**, 405 (2001).
[39] F. M. Izrailev and A. A. Krokhin, Phys. Rev. Lett. **82**, 4062 (1999).